The current issue and full text archive of this journal is available at
www.emeraldinsight.com/0961-5539.htm

Network modelling of unsteady natural convection flow over a vertical plate submitted to surface temperature oscillation

Joaquín Zueco
Department of Thermal Engineering and Fluids, Technical University of Cartagena, Cartagena, Spain

Received 2 February 2007
Revised 29 November 2007
Accepted 4 February 2008

Abstract

Purpose – The unsteady natural convection flow of a viscous dissipative fluid along a semi-infinite vertical plate subjected to periodic surface temperature oscillation is investigated.
Design/methodology/approach – An electrical-network model based on the Network Simulation Method is developed to solve the governing equations. The accuracy and effectiveness of the method are demonstrated.
Findings – The increasing of the viscous dissipation and the decreasing in the Prandtl number lead to a decrease in Nusselt number and an increase in the local skin-friction. Also, it is found that the oscillations of the Nusselt number and of the local skin-friction depend on the frequency and amplitude of the oscillating surface temperature. For Pr = 1,000 and $\varepsilon = 0.005$ (realistic case) the effect of the viscous dissipation is appreciable at large distances from the leading edge.
Research limitations/implications – The inclusion of viscous dissipation in the energy equation, except of the theoretical interest, has applications in very special cases, for example, gases at very low temperature and also for high Prandtl number liquids.
Originality/value – The influence of the non-uniformity of wall temperature on the heat transfer by natural convection along of the plate together with the viscous dissipation of the fluid are analysed by means of a new numerical technique based on the electrical analogy.
Keywords Convection, Oscillations, Temperature, Modelling, Flow
Paper type Research paper

Nomenclature

C	= capacitor	L	= height of the plate
C_{fx}	= local skin-friction coefficient	N	= number of cells
c_p	= specific heat	Nu_x	= local Nusselt number
k	= thermal conductivity	Pr	= Prandtl number
g	= acceleration due to gravity	R	= resistor
G	= control-voltage current-source	t	= time
Gr	= Grashof number	T	= temperature
Gr_x	= local Grasfof number	u, v	= velocities
h	= heat transfer coefficient	U, V	= dimensionless velocities
j	= flux density	x	= vertical co-ordinate
J	= electric current	X	= dimensionless vertical co-ordinate

The author is grateful to the reviewers for their excellent comments which helped to improve the paper.

International Journal of Numerical Methods for Heat & Fluid Flow
Vol. 19 Nos. 3/4, 2009
pp. 285-302

0961-5539
DOI 10.1108/09615530910938290

y = horizontal co-ordinate

Y = dimensionless horizontal co-ordinate

z = constant

Greek symbols

α = diffusivity thermal

β = thermal expansion coefficient

γ = dimensionless amplitude

ε = dissipation parameter

θ = dimensionless temperature

μ = dynamic viscosity

ρ = density

τ = dimensionless time

τ_w = local wall shear stress

υ = kinematic viscosity

ω = frequency

Ω = dimensionless frequency

ΔX = axial thickness of the cell

ΔY = radial thickness of the cell

Subscripts

c = characteristic

i = associated with i nodal point

j = associated with j nodal point

i, j = associated to the centre on the cell

max = maximum

w = wall

∞ = ambient

Introduction

In recent decades, many authors have solved this classical problem, Ostrach (1953) with a vertical isothermal plate or Sparrow and Gregg (1956) with a uniform flux plate, due to its relevance in a wide range of industrial applications, such as electronic components, furnaces, finned cooling surfaces, solar collectors and others. This problem is generally non-similar and only there are only a few exceptions for some particular boundary conditions at the wall, uniform surface heat flux, Sparrow and Gregg (1956), temperature variations of the power and exponential form, Sparrow and Gregg (1958), and a line source on an adiabatic plate, Jaluria and Gebhart (1977), where analytical approaches can be used, so, it is usually necessary to solve a set of coupled non-linear partial differential equations numerically.

The problem of steady-free convection heat transfer from a plate with an arbitrary surface temperature variation was solved by Kao *et al.* (1977) using methods of local similarity and local non-similarity. They employed the strained coordinates method by means of the transformation of the axial coordinate by using an integral function of the proposed wall temperature to estimate the wall heat transfer. Lee and Yovanovich (1993) solved this problem by means an approximate method based on a linearization of the conservation equations through the use of an effective velocity. They showed the potential capability of approximate techniques for problems of this type. Yang *et al.* (1982) solved the problem with beside surface heat-flux variations, applying appropriate coordinate transformations using a Merk-type series solution. They obtained a set of ordinary differential equations which they later were solved numerically by means of an iterative procedure. Harris *et al.* (1998) investigated the transient free convection from a vertical plate when the plate temperature is suddenly changed, obtaining an analytical solution (for small values time) and a numerical solution for times before the steady-state is reached. Polidori *et al.* (2003) proposed a theoretical approach to the transient dynamic behaviour of a natural convection boundary layer flow when a step variation of the uniform heat flux is applied, using the Karman–Pohlhausen integral method.

However, the class of fully numerically methods is the most versatile for handling general boundary conditions, and is capable of providing solutions very close to exacts

solutions. Havet and Blay (1999) employed a linearly varying temperature distribution to study the non-uniformity of wall temperature on heat transfer by steady turbulent free convection by means of a numerical model based on a finite-volume formulation. These numerical methods are necessary to solve the problems with surface temperature oscillation in transient natural convection from a vertical plate. In the works of Rees (1999) and Li *et al.* (2001), the surface temperature profile oscillates with the distance along the plate. Rees (1999) used a combined numerical and asymptotic analysis to study in detail how sinusoidal surface temperature profiles in the streamwise direction modify the otherwise self-similar steady boundary layer flow. For the steady problem with small values of the Grashof number the perturbation method is employed and an asymptotic solution obtained. The numerical methods for both the solution of the steady and the unsteady flow cases are obtained with Fourier series expansion. Li *et al.* (2001) developed numerical methods using an unsteady approach. In the paper of Saeid (2004), the surface temperature profile oscillates with time. This author solved the governing equations numerically using the finite-difference method, and analysed the effect of the amplitude and frequency of the oscillating surface temperature.

Other authors have studied different cases of natural convection, so Ho and Tu (1999) studied the transition into oscillatory natural convection of cold water in a 2-D vertical rectangular enclosure by means of a finite-difference method. Aydin and Yang (2000) solved numerically the problem of natural convection in an enclosure with localized heating from below and symmetrical cooling from the sides. Hossain *et al.* (2002) solved the problem of free convection flow along a vertical circular cone with uniform surface temperature and surface heat flux in a thermally stratified medium using three distinct methodologies. The finite-element method was used by Cruchaga and Celentano (2003) to study the natural and mixed convection in obstructed channels.

In the above papers, the viscous dissipation term in the energy equation was not considered. The viscous dissipation term is always positive and represents a source of heat due to friction between fluid particles. A variety of expressions are used in the literature for this term like viscous heating, shear-stress heating and viscous work. Gebhart (1962) was the first who studied this problem, taking into account the viscous dissipation and defining the typical non-dimensional dissipation parameter, $\varepsilon = g\beta L/c_p$. This number is a completely independent parameter. It has no correspondence with the Prandtl number not with the Grashof number. Almost all free convection studies are realised at an ambient temperature of 300 K at 1 atm pressure and at terrestrial gravity, in this case, the viscous dissipation is neglected in the energy equation, for most gases and low and moderate Prandtl number liquids. However, in processes wherein the scale of the process is very large, e.g. on larger planets, in large masses of gas in space, and in geological processes in fluids internal to various bodies is important the viscous dissipation effects. Also, for high gravity, for example in gas turbine blade cooling applications, where the intensity of the body force may be as large as 10^4 g, the viscous dissipation effect may affect transport even at small downstream distances from the leading edge, see Joshi and Gebhart (1981). It is possible causes a 20 per cent reduction in heat transfer in gases and in common liquids. Finally, at low temperatures for gases and for high Prandtl number liquids may be quite significant the viscous dissipation effects. In the previous cases, the viscous dissipation tends to rise the fluid temperature and this effect has a strong influence on the results as it assists the upward flow and opposes the downward flow.

Takhar *et al.* (1997) solved the problem transient natural in laminar boundary layers over a semi-infinite vertical plate with power-law variation of wall temperature. Soundalgekar *et al.* (1999), using an implicit finite-difference technique, studied the effect of the dissipation parameter on the time needed to reach steady-state in the transient free convection flow in a vertical plate, being this time different in function of the value of viscous dissipation parameter. They demonstrated that there is a rise in the average skin-friction and a fall in the average Nusselt number due to greater viscous dissipative heat. Pantokratoras (2005) solved the problem in stationary situation using the finite-difference method, with isothermal and uniform flux boundary conditions in the wall taking into account the viscous dissipation. He confirmed that the viscous dissipation has a strong influence on the results as it assists the upward flow and opposes the downward flow.

Gokhale and Al Samman (2003) studied the effects of mass transfer and viscous dissipation on the transient free convection flow of a dissipative fluid along a semi-infinite vertical plate with constant heat flux. They confirmed that the time required to reach steady-state is affected of the presence or not of viscous dissipation. In the presence of viscous dissipative heat, more time is required to reach the steady-state temperature and velocity than that in the absence of viscous dissipation. Chen (2004) solved the problem of combined heat and mass transfer in MHD free convection flow of an electrically conducting fluid along a vertical surface with Ohmic heating and viscous dissipation. He verified that when the viscous dissipation effect is included, a considerable reduction in the heat transfer rate occurs, but only slight effects on wall shear stress are observed.

In this work, the Network Simulation Method (NSM hereafter) is used as the numerical technique, firstly a spatial discretization is applied to the transient boundary-layer equations, and a set of ordinary differential equations are obtained, one for each control volume; later, by applying the electro-thermal analogy, the network model is obtained, which can be solved by means of a very common program used to simulate electrical circuits, *Pspice* (MicroSim, 1994). Today, several graphical interfaces are available to simplify code generation, with a user interface to view the results (any voltage or current waveform) of the simulation. This program calculates these voltages and currents vs time (transient analysis) or vs frequency (alternating current analysis). Moreover, *Pspice* also performs other analyse, such as direct current, sensitivity, noise and distortion.

The method does not require convergence criteria to solve the finite-difference equations resulting from discretization of the partial difference equations of the mathematical model, since *Pspice* does this work; moreover, time remains as a continuous variable in the model, only requiring finite-difference schemes for the spatial variable. NSM has been successfully applied to solving several heat transfer problems: see Alhama *et al.* (2003) for unsteady heat flux wall estimations, and Zueco *et al.* (2004) for applications to the laminar flow of fluids in ducts, Zueco and Alhama (2006) developed an iterative algorithm for the estimation of the temperature-dependent emissivity of solid metals, while Zueco and Campo (2006) solved the transient radiative transfer between the thick walls of an enclosure by means of a new network model.

The objective of the present paper is to solve the transient natural convection along a semi-infinite vertical plate subjected to periodic surface temperature oscillation problem taking into account viscous dissipation, using a new method, and to discuss of

the advantages and disadvantages of the same. The results obtained and the effect of the viscous parameter, frequency and amplitude of surface temperature are analysed.

Mathematical model

The quiescent ambient fluid around the plate is at a lower constant temperature, T_∞, with u and v denoting, respectively, the velocity components in the x and y direction, where x is vertically upwards and y is the coordinate perpendicular to x. Under the usual Boussinesq's approximation, the transient two-dimensional flow can be shown to be governed by the following boundary layer equations (including viscous dissipation),

Continuity equation:

$$\frac{\partial u}{\partial x}+\frac{\partial v}{\partial y}=0 \tag{1}$$

Momentum equation:

$$\frac{\partial u}{\partial t}+u\frac{\partial u}{\partial x}+v\frac{\partial u}{\partial y}=\beta g(T-T_\infty)+\upsilon\frac{\partial^2 u}{\partial y^2} \tag{2}$$

Energy equation:

$$\frac{\partial T}{\partial t}+u\frac{\partial T}{\partial x}+v\frac{\partial T}{\partial y}=\alpha\frac{\partial^2 T}{\partial y^2}+\frac{\upsilon}{c_{\mathrm{p}}}\left(\frac{\partial u}{\partial y}\right)^2 \tag{3}$$

with the following initial and boundary conditions:

$$t\le 0; u=0, v=0, T=T_\infty \tag{4a}$$

$$t>0; u=0, v=0, T=T_\infty \quad \text{at } x=0 \tag{4b}$$

$$t>0; u=0, v=0, T=T_{\mathrm{w}}+\gamma(T_{\mathrm{w}}-T_\infty)\sin\omega t \quad \text{at } y=0 \tag{4c}$$

$$t>0; u=0, T\to T_{\infty,} \quad \text{as } y\to\infty \tag{4d}$$

where it is considered that the boundary condition of the wall temperature is oscillating periodically over an average value T_{w} with frequency ω and amplitude γ. The above equations are written in a non-dimensional form by employing the following boundary layer dimensionless variables:

$$\mathrm{U}=u\mathrm{L}\frac{\mathrm{Gr}^{-1/2}}{\upsilon}, \mathrm{V}=v\frac{\mathrm{Gr}^{-1/4}\mathrm{L}}{\upsilon}, \mathrm{X}=\frac{x}{\mathrm{L}}, \mathrm{Y}=y\frac{\mathrm{Gr}^{1/4}}{\mathrm{L}}, \tau=t\upsilon\frac{\mathrm{Gr}^{1/2}}{\mathrm{L}^2},$$
$$\theta=\frac{T-T_\infty}{T_{\mathrm{w}}-T_\infty} \tag{5}$$

where L is the wall height, $\mathrm{Gr}=g\beta\mathrm{L}^3(T_{\mathrm{w}}-T_\infty)/\upsilon^2$ is the Grashof number. Then the governing equations reduce to the following non-dimensional boundary layer equations:

$$\frac{\partial U}{\partial X}+\frac{\partial V}{\partial Y}=0 \tag{6}$$

$$\frac{\partial U}{\partial \tau}+U\frac{\partial U}{\partial X}+V\frac{\partial U}{\partial Y}=\theta+\frac{\partial^2 U}{\partial Y^2} \tag{7}$$

$$\frac{\partial \theta}{\partial \tau}+U\frac{\partial \theta}{\partial X}+V\frac{\partial \theta}{\partial Y}=1/\mathrm{Pr}\frac{\partial^2 \theta}{\partial Y^2}+\varepsilon\left(\frac{\partial U}{\partial Y}\right)^2 \tag{8}$$

where $\mathrm{Pr}=\upsilon/\alpha$ is the Prandtl number and $\varepsilon=g\beta L/c_p$ the factor that determines the influence of viscous dissipation. The dimensionless initial and boundary conditions become:

$$\tau \le 0; U=0, V=0, \theta=0 \tag{9a}$$

$$\tau > 0; U=0, V=0, \theta=0 \quad \text{at } X=0 \tag{9b}$$

$$\tau > 0; U=0, V=0, \theta=1+\gamma\sin(\Omega\tau) \quad \text{at } Y=0 \tag{9c}$$

$$\tau > 0; U=0, \theta \to 0 \quad \text{as } Y \to \infty \tag{9d}$$

Taking the length of the semi-infinite plate as $L=1$, it consider a rectangular region with X varying from 0 to 1 and y varying from 0 to $Y_{max}=15$, where $X=L$ corresponds to the height of the plate and Y_{max} is regarded as ∞. It is ensured that Y_{max} lies well outside the momentum and thermal boundary layers. It is necessary to divide the rectangular region into Z and W grid-spacing respectively. After experimenting with a few sets of mesh sizes, a region of integration of 40×80 has been used.

Numerical procedure

The method used to solve the problem is the NSM. The discretization of the boundary-layer equations is based on the finite-difference formulation, only a discretization of the spatial co-ordinates being necessary, while time remains as a real continuous variable. The user does not need to manipulate the finite-difference differential equations to be solved nor to pay attention to the convergence problems, and there are no prerequisites as regards the time-step required for the convergence since the code Pspice imposed and adjusted continuously automatically this parameter to reach a convergent solution in each iteration, according to the given stability and convergence requirements. If a time-step solution does not converge, the time-step usually can be reduced until the solutions converge. This time-step reduction is necessary to maintain a reasonable level of truncation error in the analysis. Details of the local truncation errors can been found in the thesis of Nagel (1975). However, it is possible to indicate to the program the value maximum of the time-step ($\Delta\tau_{max}$), so that the time-step could be smaller than this value but never larger. As this value decreases, the accuracy increases and the internal computation speed decreases.

Transient analysis requires a numerical integration algorithm and a method of dynamically varying the integration time-step to maintain reasonable solution accuracy. Pspice uses the numerical implicit integration formulae (trapezoidal integration and Gear's method) with second order accuracy. The trapezoidal integration is one of the most popular ones in network transient analysis, due to its merits of low distortion and absolute stability (A-stability).

Based up on these equations, an electrical network circuit, whose equations are formally equivalent to the discretized equations is designed. The electric-thermal analogy can be applied to the equations continuity, momentum and energy, so that the variables velocities (U, V) and temperature (θ) are equivalent to the variable voltage, while the velocity fluxes (∂U/∂X, ∂U/∂Y, ∂V/∂X) and the heat flux are equivalent to the variable electric current (J). NSM simulates the behaviour of unsteady electric circuits by means of resistors, capacitors and non-linear devices that seek to resemble thermal systems governed by unsteady linear or non-linear equations. Another noticeable advantage of the NSM is that it provides both the temperature and heat flux density fields immediately (without no need numerical manipulation).

The whole network must be converted into a suitable program that is solved by a computer code in a PC using suitable software, *Pspice* (MicroSim, 1994) in this case. The latest version of this simulator adds a completely new solver to the *Pspice* simulation engine, which uses sophisticated algorithms to increase simulation speed, particularly for larger circuits with substantial run times; a also it has slightly improved convergence characteristics. This means that greater speed and better convergence can be attained without sacrificing the accuracy that is normally associated with *Pspice*.

Among the advantages of the proposed numerical method are:

- time remains as a continuous variable in the model, so, only finite-difference schemes are required for the spatial variable;
- there are no prerequisites as regards the time-step required for the convergence;
- generally, few programming rules (and few devices) are necessary since the number of the electrical devices that make up the network is very small (resistances, condensers and current sources), as is the computation time, so that it is very simple to represent any electrical circuit;
- it provides the temperature, velocities, gradients of velocity and temperature (heat flux) fields immediately;
- a wide library of electrical components is available for the future simulation of more complex processes;
- finally, other additional advantage is that the theorems of conservation and uniqueness of the flow and potential electrical variables (Kirchhoff laws), are satisfied in the circuits, some of the equations that normally are inside of the mathematical model no need to be considered for the design of the network model, for example in the conservation of the heat flux in the boundary of two different media and the uniqueness of the temperature in the boundary.

However, the design of the model requires a knowledge of circuit theory fundamentals and *Pspice* does not allow data visualization during simulation. However, to help the user a program in C++ (easy and fast to understand) was developed, so that the user uses it without spending a lot of time in the implementation of the code *Pspice* (file "oscillation.cir"). This program generates quickly the file for his later execution in *Pspice*, and the program permits the reading of the solutions provided by *Pspice* (file "oscillation.out") in any position and to any time. Besides, after completing the simulation, *Pspice* plots waveform results so the designer can visualize circuit behaviour and determine design validity. Graphical results of each simulation are presented in *Pspice's* Probe window waveform viewer and analyser, where it is possible

to see the temporal evolution of velocities, temperatures, skin-friction and Nusselt number any point of the medium. Basically, the NSM uses the most recent advances in software in the resolution of electrical networks to apply to different kinds of partial differential equations: elliptical, hyperbolical and parabolic; linear and non-linear, in 1D, 2D and 3D, typical in problems of fluids mechanics or heat transfer.

Alhama (1999) established the connection between the total number of volume elements (N) and the accuracy of the NSM. For $N \geq 30$ for vertical and horizontal directions, numerical errors are reduced to values below 0.5 per cent nearly along the whole transient period for 2-D problems. The maximum value of the time-step is $\Delta\tau_{max} = 0.05\,s$ for the isothermal wall case, and $\Delta\tau_{max} = 0.005\,s$ for the oscillation surface temperature case. Computational times for the same type of problems are comparables (ever minor) to the other numerical techniques general. This time depends principally of the accuracy wished, spatial grid and of the $\Delta\tau_{max}$. The computational time maximum is about of 120 s ($\Delta\tau_{max} = 0.005\,s$) and the time minimum of 6 s ($\Delta\tau_{max} = 0.05\,s$).

Design of the network model

The finite-difference differential equations resulting from dimensionless continuity, momentum balance and energy equations are obtained in this section. A second-order central difference scheme has been used to discretize the boundary layers equations and the resulting system of finite-difference equations are solved employing the *Pspice* program.

$$\left(\frac{\partial U}{\partial Y}\right)_{i,j} \approx \frac{(U_{i,j+1} - U_{i,j-1})}{(2\Delta Y)} \tag{10}$$

$$\left(\frac{\partial^2 U}{\partial Y^2}\right)_{i,j} \approx \frac{(U_{i,j+1} + U_{i,j-1} - 2U_{i,j})}{\Delta Y^2} = \frac{1}{\Delta Y}\left[\frac{(U_{i,j-1} - U_{i,j})}{\Delta Y} - \frac{(U_{i,j} - U_{i,j+1})}{\Delta Y}\right] \tag{11}$$

For the variable X is used a central difference too. The terms "$(U_{i,j-1} - U_{i,j})/\Delta Y$" and "$(U_{i,j} - U_{i,j+1})/\Delta Y$" represent the electrical currents, $J_{U,i,j-\Delta Y}$ and $j_{U,i,j+\Delta Y}$, respectively. They can be modelled by means of two resistor of value "ΔY" between the extremes of $U_{i,j-1}$, $U_{i,j}$ and $U_{i,j}$, $U_{i,j+1}$, respectively. However, it is realised a major discretization, so each resistor is divided into two of values "$\Delta Y/2$", accord to the expressions following,

$$\begin{aligned}\left(\frac{\partial^2 U}{\partial Y^2}\right)_{i,j} &\approx \frac{1}{\Delta Y}\left[\frac{(U_{i,j-1} - U_{i,j-\Delta Y})}{(\Delta Y/2)} - \frac{(U_{i,j-} U_{i,j+\Delta Y})}{(\Delta Y/2)}\right] \\ &= \frac{1}{\Delta Y}\left[\frac{(U_{i,j-\Delta Y} - U_{i,j})}{(\Delta Y/2)} - \frac{(U_{i,j+\Delta Y} - U_{i,j+1})}{(\Delta Y/2)}\right]\end{aligned} \tag{12}$$

where $U_{i,j-\Delta Y}$ and $U_{i,j+\Delta Y}$ are the points extremes of the elemental cell i, j. Figure 1 shows the physical medium reticulation with elementals cells connected between them, where it is possible observed that the thickness of the elemental cell is ΔY. This connecting requires, equal potentials at the contact points of adjoining cells and equal outward–inward transference flows in adjoining elements. Therefore, the finite-difference differential equations are,

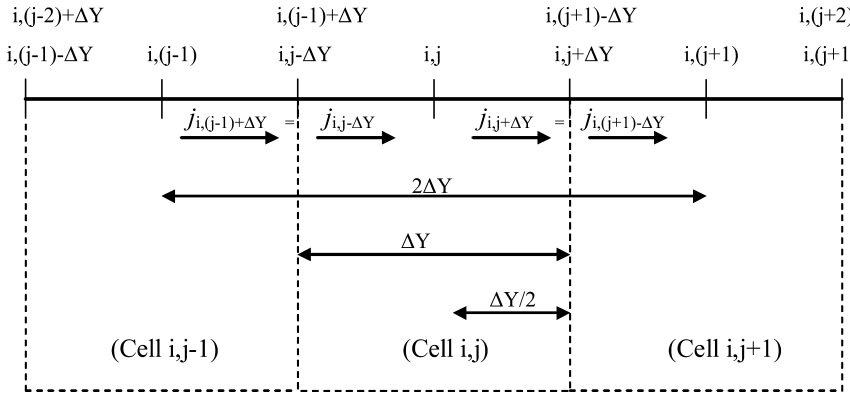

Figure 1.
Grid system used

$$\Delta Y\frac{dU_{i,j}}{d\tau}+\Delta YU_{i,j}\frac{(U_{i+\Delta X,j}-U_{i-\Delta X,j})}{\Delta X}+V_{i,j}(U_{i,j+\Delta Y}-U_{i,j-\Delta Y})$$
$$=\Delta Y\theta_{i,j}+\frac{(U_{i,j-\Delta Y}-U_{i,j})}{(\Delta Y/2)}-\frac{(U_{i,j}-U_{i,j+\Delta Y})}{(\Delta Y/2)} \quad (13)$$

$$\Delta YPr\frac{d\theta_{i,j}}{d\tau}+\Delta YPrU_{i,j}\frac{(\theta_{i+\Delta X,j}-\theta_{i-\Delta X,j})}{\Delta X}+PrV_{i,j}(\theta_{i,j+\Delta Y}-\theta_{i,j-\Delta Y})$$
$$=\frac{(\theta_{i,j-\Delta Y}-\theta_{i,j})}{\Delta Y/2}-\frac{(\theta_{i,j}-\theta_{i,j+\Delta Y})}{\Delta Y/2}+\varepsilon Pr\frac{(U_{i,j+\Delta Y}-U_{i,j-\Delta Y})^2}{\Delta Y} \quad (14)$$

Equations (13) and (14) can be written in the form of Kirchhoff's law,

$$j_{U,i,j+\Delta Y}-j_{U,i,j-\Delta Y}-j_{U,i,j}+j_{Ux,i,j}+j_{Uy,i,j}+j_{Uc,i,j}=0 \quad (15)$$
$$j_{\theta,i,j+\Delta Y}-j_{\theta,i,j-\Delta Y}-j_{\theta,i,j}+j_{\theta x,i,j}+j_{\theta y,i,j}+j_{\theta c,i,j}=0 \quad (16)$$

Figure 2 shows the network models corresponds to the Equations (15) and (16). In the Figure 2a, $j_{U,i,j+\Delta Y}$ and $j_{U,i,j-\Delta Y}$ are the currents that leave and enter the cell for the friction term of U, $j_{U,i,j}$ the current due to the buoyancy term, $j_{Ux,i,j}$ and $j_{Uy,i,j}$ are the currents due to the inertia terms of U and V, respectively, while $j_{Uc,i,j}$ is the transitory term. The currents $j_{U,i,j+\Delta Y}$ and $j_{U,i,j-\Delta Y}$ are implemented by means of two resistances $R_{U,i,j\pm\Delta Y}$ of values "$\Delta Y/2$"; while the currents $j_{U,i,j}$, $j_{Ux,i,j}$ and $j_{Uy,i,j}$ are implemented by means of voltage control current generators, $G_{U,i,j}$, $G_{U,\Delta X,i,j}$ and $G_{U,\Delta Y,i,j}$, respectively; these voltages are "$\Delta Y\ \theta_{i,j}$", "$\Delta Y\ U_{i,j}\ (U_{i+\Delta X,j}-U_{i-\Delta X,j})/\Delta x$" and "$V_{i,j}\ (U_{i,j+\Delta Y}-U_{i,j-\Delta Y})$", respectively; with $U_{i+\Delta X,j}$, $U_{i-\Delta X,j}$, $U_{i,j+\Delta Y}$ and $U_{i,j-\Delta Y}$ being the voltages (velocities) of the nodes "$i+\Delta X,j$", "$i-\Delta X,j$", "$i,j+\Delta Y$" and "$i,j-\Delta Y$" in the cell of the momentum equation, while $U_{i,j}$ is the velocity in the centre of this cell (i,j). $j_{Uc,i,j}$ is implemented by means a capacitor $C_{U,i,j}$ of value "ΔY", connected to the centre of each cell. For the energy equation, similar explanations can be realised to the previous case. The devices that integrate the network model are the same (Figure 2b), only the actions of control on the current generators are modified and the value of the condenser. In this case variable voltage corresponds with the temperature.

Finally, to implement the boundary conditions are employed the following devices are used:

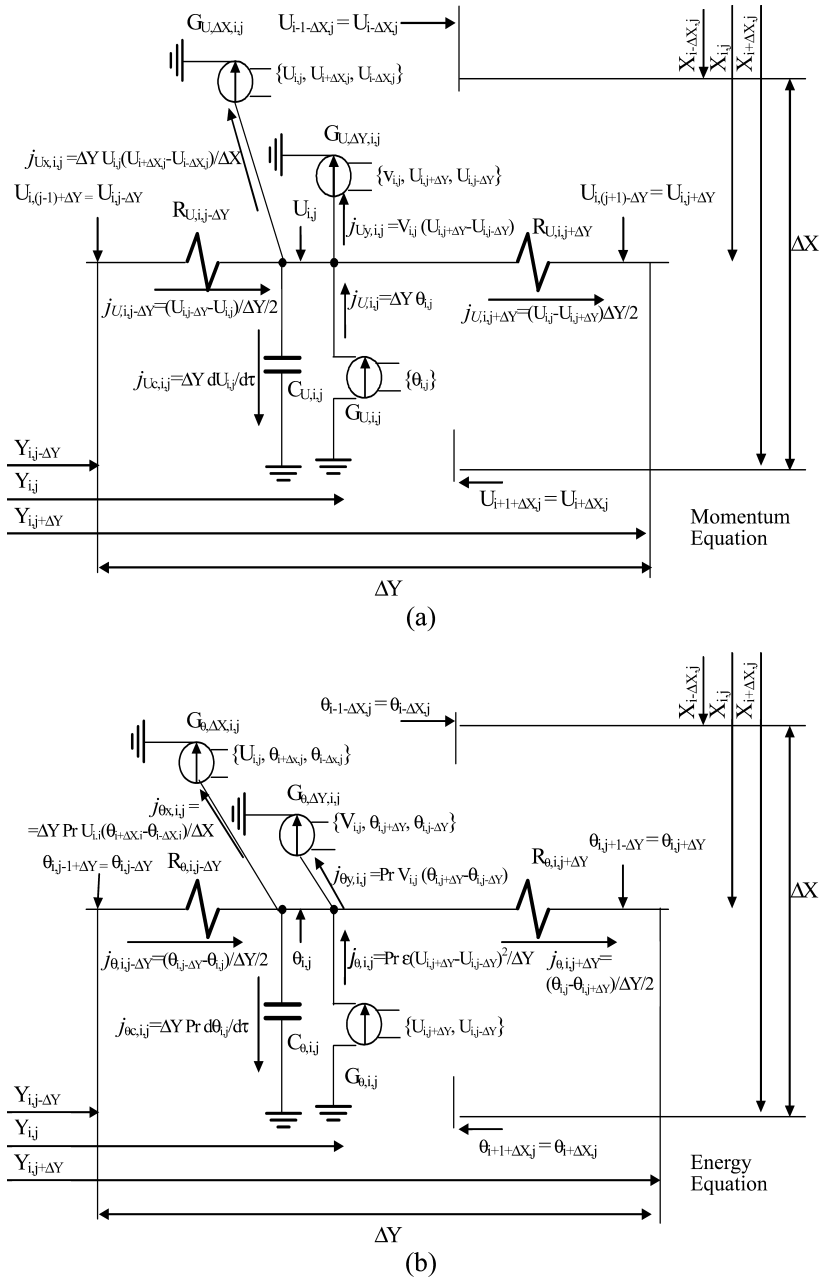

Figure 2.
Nomenclature and network model of the control volume: (a) momentum balance equation and (b) energy balance equation

- a voltage-source for the constant values of velocity and temperature; and
- a sinusoidal voltage-source for the sinusoidal temperature variation. As regards the initial condition, the voltages $U = 0$ and $\theta = 0$ are applied to the capacitors $C_{U,i,j}$ and $C_{\theta,i,j}$.

From the finite-difference equation corresponding to Equation (1) the velocity component $V_{i,j}$ is obtained explicitly:

$$V_{i,j} = V_{i,j-1} + \frac{(U_{i-\Delta X,j} - U_{i,j})\Delta Y}{(2\Delta X)} \text{ for } X = 0 \quad (17a)$$

$$V_{i,j} = V_{i,j-1} + \frac{(U_{i-\Delta X,j} - U_{i+\Delta X,j})\Delta Y}{\Delta X} \text{ for } X > 0 \quad (17b)$$

Results and discussion

Figure 3(a) and (b) shows the transient and steady-state velocity profiles (U) and temperature profiles (θ) at the upper end of the wall (X = 1), for air (Pr = 0.72) with no viscous dissipation considered ($\varepsilon = 0$) and a constant temperature wall ($\theta_w = 1$). These figures also show the results obtained by Saeid (2004) for comparison. The excellent degree of agreement of the present results with those of this author using a fully implicit finite-difference scheme, can be appreciated. We observe from this figure that both velocity and temperature increase with time to reach maximum values and then decrease to reach the steady-state. To obtain the steady-state, the condenser of the network merely has to be omitted.

For practical applications, the principal physical quantities of interest in heat transfer include the local skin-friction coefficient $C_{fx} = \tau_w/\rho u_c^2$ (with τ_w the local wall

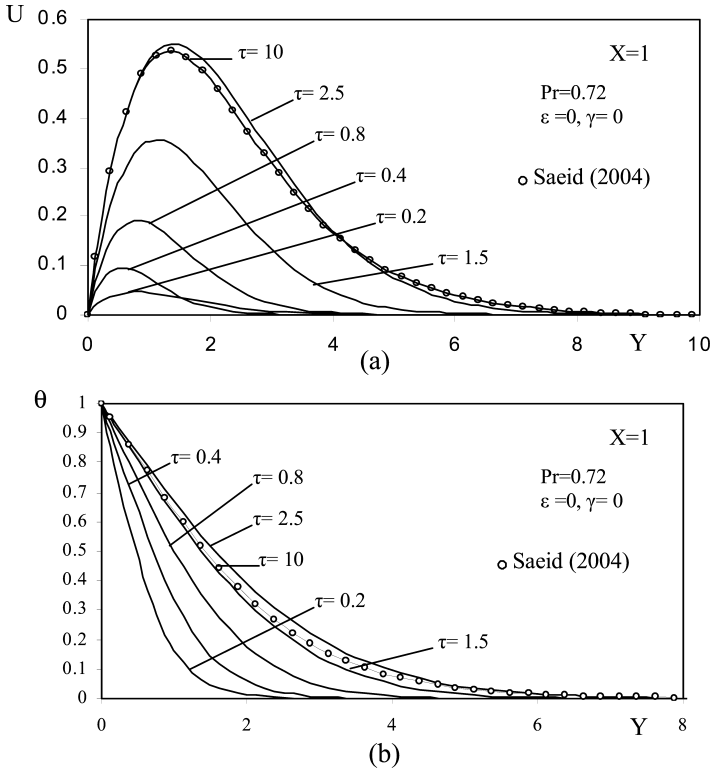

Figure 3.
Velocity and temperature profiles for air (Pr = 0.72) at X = 1, $\varepsilon = \gamma = 0$, for various values of τ: (a) dimensionless velocity profiles and (b) dimensionless temperature profiles

shear stress) and the local Nusselt number $Nu_x = h\,x/k$, being $h = -k\,(\partial T/\partial y)_{y=0}$ the convective heat transfer coefficient. Them can been expressed as:

$$C_{fx}Gr^{3/4} = \left(\frac{dU}{dY}\right)_{Y=0} \tag{18}$$

$$Nu_x Gr_x^{-1/4} = \frac{-X^{1/4}}{\theta_w(\tau)^{5/4}}\left(\frac{d\theta}{dY}\right)_{Y=0} \tag{19}$$

where $Gr_x = g\beta x^3(T_w - T_\infty)/\upsilon^2$ is the local Grashof number.

It should be noted here that the dissipation number is small for most ordinary engineering devices with common fluids for the gravitational field strength of the earth, so $4\ 10^{-7}\,m^{-1} < g\beta/c_p < 4\ 10^{-4}\,m^{-1}$. However, gases at very low temperature (50 K) can have a high value of β/c_p and also for high Prandtl number liquids, therefore the viscous dissipation term must be included in the energy equation. The effect increasing at large values of x, but in this case is possible to have a flow turbulent. To sum up, the inclusion of viscous dissipation in the energy equation, except of the theoretical interest, has applications in very special cases cited before.

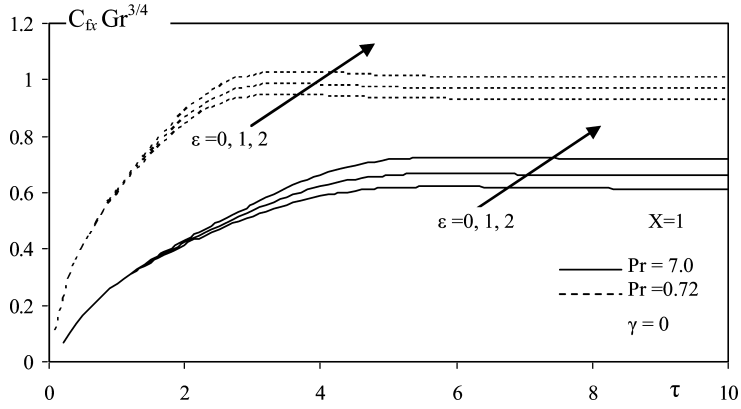

Figure 4.
Transient evolution of the local skin-friction coefficient for air (Pr = 0.72) and water (Pr = 7) at X = 1, $\gamma = 0$, $\varepsilon = 0$, 1, 2 and 3

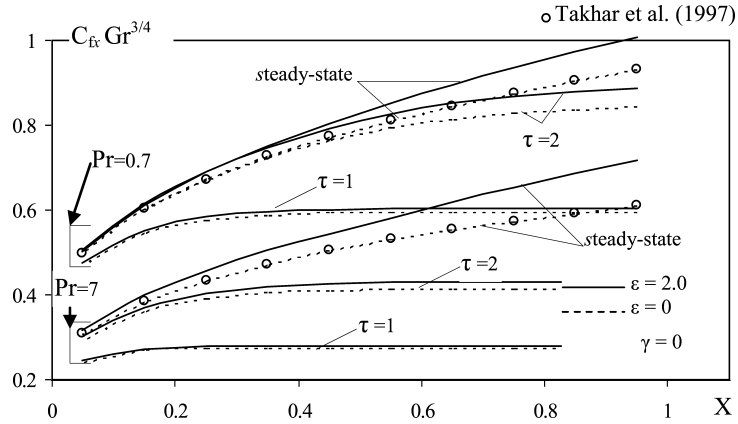

Figure 5.
Evolution axial (X-direction) of the local skin-friction coefficient for air (Pr = 0.7) and water (Pr = 7) with $\gamma = 0$, $\varepsilon = 0$ and 2, for various values of τ

Figure 4 shows the transient evolution of the local skin-friction coefficient ($C_{fx}\,Gr^{3/4}$) for the air (Pr = 0.72) and the water (Pr = 7) for X = 1, with constant wall temperature ($\theta_w = 1$ or $\gamma = 0$) and various values of the dissipation parameter ($\varepsilon = 0$, 1 and 2). It can be seen that an increase of the Prandtl number leads to a decrease in local skin-friction. Beside, greater viscous dissipative heat causes a rise in the local skin-friction.

Figure 5 shows the axial evolution (X-direction) of the local skin-friction coefficient for the air (Pr = 0.7) and the water (Pr = 7) with $\gamma = 0$, $\varepsilon = 0$ and 2, for various values of dimensionless time. This figure also shows the results obtained by Takhar *et al.* (1997) for comparison, being the almost identical results. The local skin-friction coefficient increases with time to reach a maximum. This figure confirms that the decrease in local skin-friction with increasing Pr and the increase in the local skin-friction with increased viscous dissipative heat occurred in all points of the wall (all values of X).

Figure 6 show the periodic oscillation of the local skin-friction coefficient for the air (Pr = 0.72) at X = 1, with a frequency $\Omega = 5$, two values of amplitude ($\gamma = 0.1$ and 0.5) and various values of $\varepsilon = 0$, 0.5 and 1. Greater local skin-friction can seen at the upper end of the wall (X = 1). Beside, an increase in the amplitude leads to an increase of the local skin-friction extreme (maximum and minimum) values. However, it is also

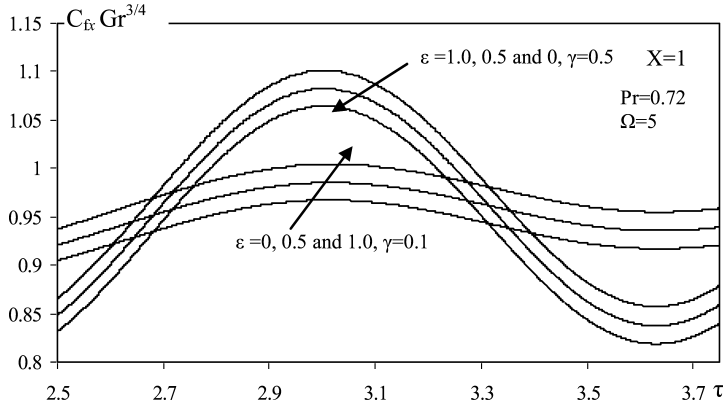

Figure 6.
Periodic oscillation of the local skin-friction coefficient for third period, air (Pr = 0.72) with, $\Omega = 5$, $\gamma = 0.1$ and 0.5, $\varepsilon = 0$, 1 and 2 at X = 1

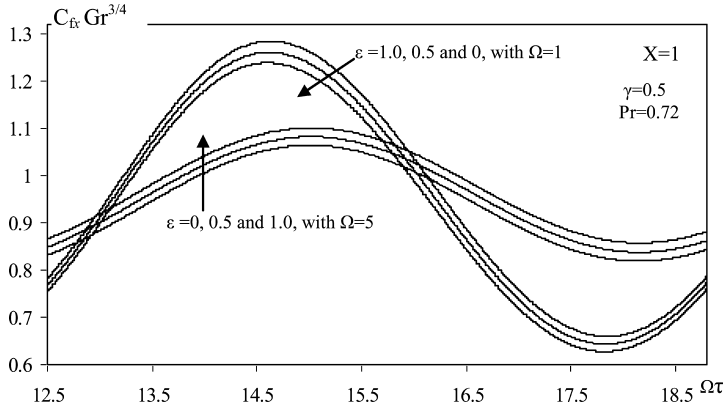

Figure 7.
Periodic oscillation of the local skin-friction coefficient with $\Omega\tau$ for third period, air (Pr = 0.72) with, $\gamma = 0.5$, $\varepsilon = 0$ and 2, $\Omega = 1$, 2 and 5 at X = 1

possible that for the same value of τ and ε, the local skin-friction will be greater for a lower γ. It is observed (as in Figure 4) that greater viscous dissipative heat causes a rise in local skin-friction, but is proportionally greater as X increases.

Figure 7 shows the effect of the oscillation frequency on the local skin-friction coefficient for air (Pr = 0.72) at X = 1, with $\gamma = 0.5$, $\varepsilon = 0$, 0.5 and 1.0. Different

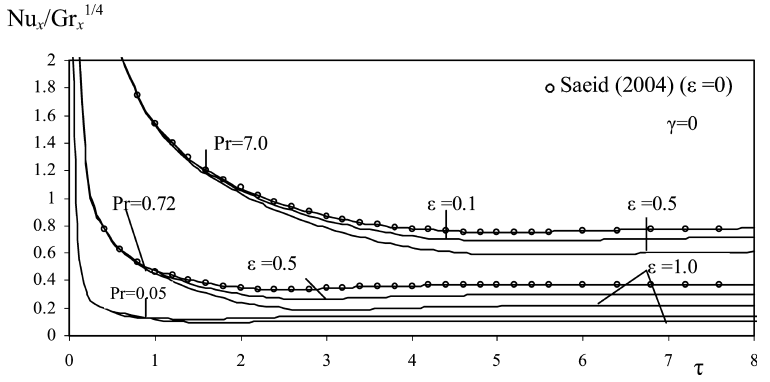

Figure 8.
Evolution of the local Nusselt number with dimensionless time for Pr = 0.05, Pr = 0.72 (air) and Pr = 7.0 (water) at X = 1, $\gamma = 0$, $\varepsilon = 0$, 0.1, 0.5 and 1.0

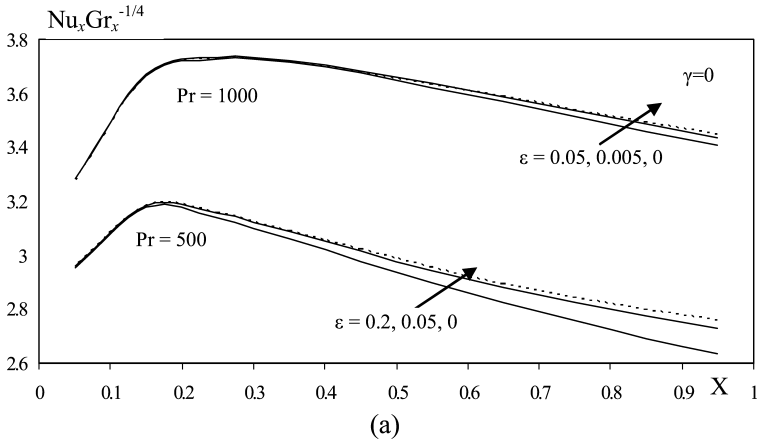

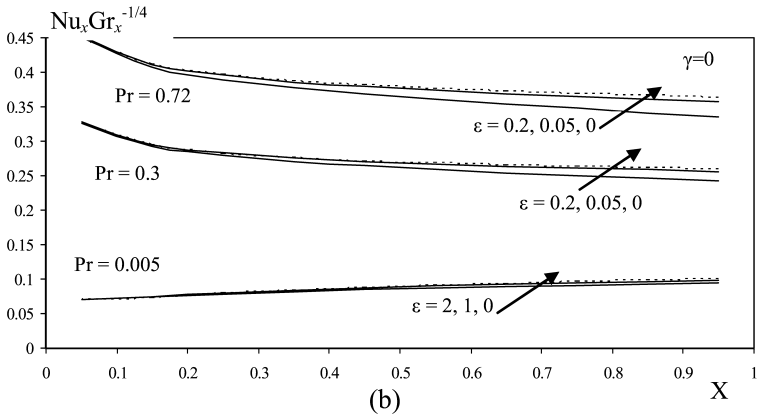

Figure 9.
Evolution of the local Nusselt number with X for $\gamma = 0$: (a) Pr = 500.0 and 1,000.0, $\varepsilon = 0$, 0.005, 0.05 and 0.2 (b) Pr = 0.005, 0.30 and 0.72, $\varepsilon = 0$, 0.005, 0.05, 0.2, 1.0 and 2.0

values (1 and 5) of Ω are employed. We can see that an increase in the frequency leads to a decrease in the local skin-friction extreme (maximum and minimum) values. However, it is also possible that for the same value of τ and ε, the local skin-friction will be greater for a higher value of Ω.

Figure 8 shows the temporal evolution of local Nusselt number for $\varepsilon = 0$, 0.1, 0.5 and 1 and Pr = 0.72 and 7.0 with constant wall temperature ($\theta_w = 1$). The figure also shows the results of Saeid (2004), for $\varepsilon = 0$; as can be seen, they are very close. The local Nusselt number decreases with time and reaches a minimum value before increasing slightly to reach the steady-state. It can be observed that an increase in the Prandtl number leads to an increase in the local Nusselt number, while an increase in viscous dissipation leads to a decrease in the local Nusselt number.

Figure 9(a) and (b) is plotted the evolution of the local Nusselt number with X for various values of Pr (0.005, 0.30, 0.72, 500.0 and 1,000.0), $\varepsilon = 0$, 0.005, 0.05, 0.2, 1.0 and 2.0, with constant surface temperature boundary condition. It is observed that greater viscous dissipative heat causes a decrease in local Nusselt number proportionally greater as X and Pr increase. It can be observed that with Pr = 1,000 and $\varepsilon = 0.005$ (realistic case) the effect of the viscous dissipation is appreciable.

Figure 10 shows the effect of the amplitude on the local Nusselt number with dimensionless time at X = 1, with Pr = 0.72 and $\Omega = 5.0$, for various values of γ (0.5 and 0.1) and of Ec (0, 0.5, 1.0 and 2.0). Note that the oscillations of $Nu_x Gr_x^{-1/4}$ are greater for high values of the amplitude; moreover, $Nu_x Gr_x^{-1/4}$ increases when γ increases. A rise in viscous dissipation heat causes a decrease in the local Nusselt

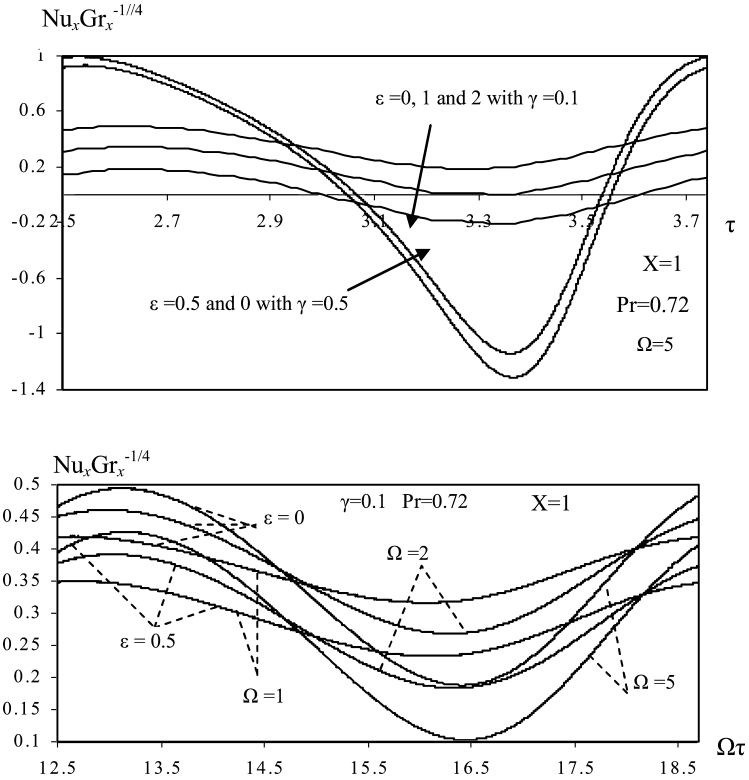

Figure 10.
Effect of the dimensionless amplitude on the local Nusselt number with dimensionless time for third period at X = 1, $\varepsilon = 0$, 1.0, 2.0 and 3.0, with Pr = 0.72, $\gamma = 0.1$ and 0.5 and $\Omega = 5.0$

Figure 11.
Effect of the frequency on the local Nusselt number at X = 1 for third period, with $\varepsilon = 0$ and 0.5, with Pr = 0.72, $\gamma = 0.1$ and $\Omega = 1.0$, 2.0 and 5.0

number, after which this parameter may become negative, which implies that there are some points in the boundary layer with temperatures higher than the surface temperature or that the viscous dissipation heat accelerates this tendency (negative values of Nusselt number always being possible if ε is high).

Figure 11 shows the effect of frequency on the local Nusselt number at $X = 1$, with $\varepsilon = 0$ and 0.5, with $Pr = 0.72$, $\gamma = 0.1$ and $\Omega = 1.0$, 2.0 and 5.0. In this figure is represented the evolution of $Nu_x Gr_x^{-1/4}$ vs $\Omega\tau$ in an oscillating period. Note that the oscillation of $Nu_x Gr_x^{-1/4}$ is more intensive for high frequency values.

Conclusions

A new numerical method based on electro-thermal analogy is proposed for the numerical solution of 2-D transient free convection flow of viscous dissipative fluid along a semi-infinite vertical plate subjected to periodic surface temperature oscillation. With this method, it is possible to visualise directly the evolution of the local and/or integrated transport variables (velocities, temperatures, fluxes) at any point or section of the medium. The time derivates are not replaced by finite differences and the good accuracy of the method arises from an appropriate approximation of the first time derivative using smoothing polynomials internal to *Pspice*.

The results are presented for the major parameters including the Prandtl number, dissipation parameter, Nusselt number, local skin-friction coefficient, non-dimensional frequency and non-dimensional amplitude. A systematic study on the effects of these parameters on flow and heat transfer characteristics is carried out, the principally deductions being the following:

- $C_{fx}\, Gr^{3/4}$ increase with a decreasing of the Prandtl number and greater viscous dissipation.
- An increase in viscous dissipation and a decrease in the Prandtl number lead to a decrease in $Nu_x Gr_x^{-1/4}$.
- An increase in the frequency of the oscillating surface temperature lead to greater oscillations of the Nussel number and a decrease of the oscillations of the local skin-friction.
- Oscillations of the local skin-friction and of the Nusselt number are more pronounced for high amplitude values.
- The inclusion of viscous dissipation in the energy equation, except of the theoretical interest, has applications in very special cases. For example, for $Pr = 1{,}000$ and $\varepsilon = 0.005$ (realistic case) the effect of the viscous dissipation is appreciable as X increases.

References

Alhama, F. (1999), "Transient thermal responses and nonlinear heat conduction process using the network simulation method", PhD thesis, University of Murcia, Murcia.

Alhama, F., Zueco, J. and González-Fernández, C.F. (2003), "An inverse determination of unsteady heat fluxes using a network simulation method", *Journal of Heat Transfer*, Vol. 125, pp. 1178-83.

Aydin, O. and Yang, W.-J. (2000), "Natural convection in enclosures with localized heating from below and symmetrical cooling from sides", *International Journal of Numerical Methods for Heat & Fluid Flow*, Vol. 10, pp. 518-29.

Chen, C.-H. (2004), "Combined heat and mass transfer in MHD free convection from a vertical surface with Ohmic heating and viscous dissipation", *International Journal Engineering Science*, Vol. 42, pp. 699-713.

Cruchaga, M. and Celentano, D. (2003), "Modelling natural and mixed convection in obstructed channels", *International Journal of Numerical Methods for Heat & Fluid Flow*, Vol. 13, pp. 57-85.

Gebhart, B. (1962), "Effects of viscous dissipation in natural convection", *Journal of Fluid Mechanics*, Vol. 14, pp. 225-32.

Gokhale, M.Y. and Al Samman, F.M. (2003), "Effect of mass transfer on the transient free convection flow of a dissipative fluid along a semi-infinite vertical plate with constant heat flux", *International Journal of Heat and Mass Transfer*, Vol. 46, pp. 999-1011.

Harris, S.D., Elliot, L., Ingham, D.B. and Pop, I. (1998), "Transient free convection flow past a vertical flat plate subject to a sudden change in surface temperature", *International Journal of Heat and Mass Transfer*, Vol. 41, pp. 357-72.

Havet, M. and Blay, D. (1999), "Natural convection over a non-isothermal vertical plate", *International Journal of Heat and Mass Transfer*, Vol. 42, pp. 3103-12.

Ho, C.J. and Tu, F.J. (1999), "Numerical study on oscillatory convection of cold water in a tall vertical enclosure", *International Journal of Numerical Methods for Heat & Fluid Flow*, Vol. 9, pp. 487-508.

Hossain, M.A., Paul, S.C. and Mandal, A.C. (2002), "Natural convection flow along a vertical circular cone with uniform surface temperature and surface heat flux in a thermally stratified medium", *International Journal of Numerical Methods for Heat & Fluid Flow*, Vol. 12, pp. 290-305.

Jaluria, Y. and Gebhart, B. (1977), "Buoyancy-induced flow arising from a line thermal source on an adiabatic vertical surface", *International Journal of Heat and Mass Transfer*, Vol. 20, pp. 153-7.

Joshi, Y. and Gebhart, B. (1981), "Effect of pressure work and viscous dissipation in some natural convection flows", *International Journal of Heat and Mass Transfer*, Vol. 24, pp. 1577-88.

Kao, T.T., Domoto, G.A. and Elrod, H.G., Jr. (1977), "Free convection along a nonisothermal vertical flat plate", *Journal of Heat Transfer*, Vol. 99, pp. 72-8.

Lee, S. and Yovanovich, M.M. (1993), "Linearization method for buoyancy induced flow over a nonisothermal vertical plate", *Journal of Thermophysics and Heat Transfer*, Vol. 7, pp. 158-64.

MicroSim (1994), *Pspice 6.0.*, MicroSim Corporation, Irvine, CA.

Nagel, L.W. (1975), *SPICE, a Computer Program to Simulate Semiconductor Circuits*, Memo UCB/ERL M520, University of California, Berkeley, CA.

Ostrach, S. (1953), "An analysis of laminar free-convection flow and heat transfer about a flat plate parallel to the direction of the generating body force", NASA TR., 1111.

Pantokratoras, A. (2005), "Effect of viscous dissipation in natural convection along a heated vertical plate", *Applied Mathematical Modelling*, Vol. 29, pp. 553-64.

Polidori, G., Popa, C. and Hoang-Mai, T. (2003), "Transient flow rate behaviour in an external natural convection boundary layer", *Mechanics Research Communication*, Vol. 30, pp. 515-621.

Rees, D.A.S. (1999), "The effect of steady streamwise surface temperature variations on vertical free convection", *International Journal of Heat and Mass Transfer*, Vol. 42, pp. 2455-64.

Saeid, N.H. (2004), "Periodic free convection from vertical plate subjected to periodic surface temperature oscillation", *International Journal of Thermal Sciences*, Vol. 43, pp. 569-74.

Soundalgekar, V.M., Jaiswal, B.S., Uplekar, A.G. and Takhar, H.S. (1999), "Transient free convection flow of viscous dissipative fluid past a semi-infinite vertical plate", *Applied Mechanics and Engineering*, Vol. 4, pp. 203-18.

Sparrow, E.M. and Gregg, J.L. (1956), "Laminar free convection from a vertical plate with uniform surface heat flux", *Journal of Heat Transfer*, Vol. 78, pp. 435-40.

Sparrow, E.M. and Gregg, J.L. (1958), "Similar solutions for free convection from a non-isothermal vertical plate", *Journal of Heat Transfer*, Vol. 80, pp. 379-84.

Takhar, H.S., Ganesan, P., Ekambanavam, K. and Soundalgekar, V.M. (1997), "Transient free convection past a semi-infinite vertical plate with variable surface temperature", *International Journal of Numerical Methods for Heat & Fluid Flow*, Vol. 7, pp. 280-96.

Yang, J., Jeng, D.R. and De Witt, K.J. (1982), "Laminar free convection from a vertical plate with nonuniform surface conditions", *Numerical Heat Transfer*, Vol. 5, pp. 165-84.

Zueco, J. and Alhama, F. (2006), "Inverse estimation of temperature dependent emissivity of solid metals", *Journal of Quantitative Spectroscopy & Radiative Transfer*, Vol. 101, pp. 73-86.

Zueco, J. and Campo, A. (2006), "Transient radiative transfer between the thick walls of an enclosure using the network simulation method", *Applied Thermal Engineering*, Vol. 26, pp. 673-9.

Zueco, J., Alhama, F. and González-Fernández, C.F. (2004), "Analysis of laminar forced convection with network simulation in thermal entrance region of ducts", *International Journal of Thermal Sciences*, Vol. 43, pp. 443-51.

Corresponding author

Joaquín Zueco can be contacted at: joaquin.zueco@upct.es